Astron. Astrophys. 305, 660–668 (1996)

ASTRONOMY AND ASTROPHYSICS

Spectral line radiation from solar small-scale magnetic flux tubes

F. Kneer[1], **S.S. Hasan**[2], **and W. Kalkofen**[1,3]

[1] Universitäts-Sternwarte, Geismarlandstr. 11, D-37083 Göttingen, Germany
[2] Indian Institute for Astrophysics, Sarjapur Road, Bangalore 560034, India
[3] Harvard-Smithsonian Center for Astrophysics, 60 Garden Street, Cambridge MA 02138, USA

Received 24 February 1995 / Accepted 6 May 1995

Abstract. We consider spectral line radiation from small-scale magnetic model flux tubes in the solar atmosphere. The structure of the tube is determined from the magnetostatic equations in the thin flux tube approximation. We assume that the tube is in energy equilibrium and pressure balance with the ambient medium. For the latter, we construct a quiet sun model with an artificial heating term in order to reproduce the VAL C model, treating the medium as a plane-parallel atmosphere. The flux tube models are parameterized by the plasma β_0 (the ratio of gas the pressure to the magnetic pressure), the convective efficiency parameter α, and the radius R_0 at height $z = 0$ (τ_{5000} =1) in the quiet sun. The Stokes I and V profiles emerging from the models and averaged over areas that include the neighbourhood of the flux tube are calculated for various spectral lines with different sensitivity for magnetic field strength and temperature. The profiles are compared with high spatial resolution observations of plages near disc centre that have been obtained with the Gregory Coudé Telescope at the Observatorio del Teide/Tenerife.

The information contained in both I and V profiles is found to be very useful in constraining the theoretical models. The best match of models with observations is achieved for values of β_0 between 0.3 and 0.5. For a sufficiently wide separation of the V extrema of the strongly split lines, a broadening mechanism is required. Pure velocity (microturbulent) broadening compatible with observations of strongly split lines gives too much broadening for weakly split lines. A broadening that is proportional to the Landé factor, i.e., magnetic broadening, appears to be more appropriate. This suggests dynamic models with temporary enhancement of the magnetic field strength. The continuum intensity of our models is higher and the absorption and V amplitude in the Fe II 6149 Å line are stronger than observed. An improvement in the match between model predictions and observations is likely to come from models in which the ambient gas has a lower temperature as well as a lower temperature gradient than are found in the quiet, field-free sun. Such models are currently under development for cylindrical flux tubes.

Send offprint requests to: F. Kneer

Key words: Sun: plages – Sun: magnetic fields – polarization

1. Introduction

Small-scale magnetic flux tubes in the solar atmosphere occur preferentially at the boundaries of supergranulation cells, outlined by the chromospheric Ca network, and in plage regions. They are important features of the solar atmosphere and have a significant influence on the structure and dynamics of the chromosphere and corona as well as the solar wind. Their field strength is empirically known to be in the kilogauss range and their diameters in the photosphere are believed to be typically in the range of 100–300 km. The value of the continuum intensity in the visible spectral range is a matter of some debate. Koutchmy (1977) determines for isolated, bright facular points near disc center of the sun an intensity that is a factor 1.6–2 higher than the average continuum intensity. Auffret & Muller (1991) find in high spatial resolution photographs from disc centre that, without correction for image deterioration, the brightness of photospheric facular points is enhanced by 8 percent on average, while Keller (1994) does not see brightening to be correlated with small-scale magnetic fields. The larger flux tubes become visible as pores, i.e., as structures that are darker than their surroundings. The reader is referred to Stenflo (1994), Schüssler & Schmidt (1994), or Solanki (1995) for recent reviews concerning flux tubes and for further references.

This contribution deals with models of cylindrical, small-scale flux tubes that have recently been constructed by Hasan & Kalkofen (1994), henceforth denoted by HK. These models have reached a level of realism that permits a comparison of computed and observed radiation fields. The models are constructed in the slender tube approximation. The tubes are in pressure balance with their ambient medium. Their temperature structure in the upper layers is determined by radiative flux from the surrounding gas, while the pressure inside the tubes is obtained from the hydrostatic equilibrium equation. The value of the plasma β, i.e., the ratio of the internal gas pressure to the

magnetic pressure, at a reference level is used to determine the topology of the magnetic field. The observations of Stokes I and V profiles used for comparison with the model calculations are those from high spatial resolution spectrograms obtained with the Gregory Coudé Telescope (GCT) at the Observatorio del Teide/ Tenerife. This comparison with high resolution observations imposes constraints on the models. For instance, we will show that intensity profiles, in addition to the V profiles, provide valuable information on the state of the gas inside and outside the flux tubes.

A similar investigation has recently been carried out by Grossmann-Doerth et al. (1994). Based on early calculations by Deinzer et al. (1984a, b), the models of these authors are dynamic in the sense that they are calculated from an initial configuration with homogeneous magnetic field which evolves to a final quasi-stationary state. In this state, there are weak oscillatory motions within the flux tube and large flows in the surrounding medium. On the periphery of the tube there is a downflow. Grossmann-Doerth et al. (1994) compared the radiation from their models with low resolution observations, which average over many solar structures with possibly very different properties. In this case, only the V profiles carry information since the main contribution of the normal solar atmosphere is to the average I profiles.

The structure of the paper is as follows: the observational aspects are discussed in Sect. 2, followed by a description of the theoretical models in Sect. 3. The calculation of the Stokes I and V profiles is given in Sect. 4. The results are presented in Sect. 5, followed by a discussion of the results and the main conclusions in Sect. 6.

2. Observations

Part of the observations used here have already been published (Amer & Kneer 1993), whereas the remainder will be discussed in greater detail in a forthcoming paper. We use high resolution spectrograms from plages near disc centre ($\sin\theta \leq 0.3$) in left- and right circularly polarized light, obtained in August 1991 (Amer & Kneer 1993) and August/September 1992 with the GCT on Tenerife. Combinations of any two of the three regions around the spectral lines Fe II 6149 Å (Landé factor $g = 4/3$), Fe I 6151 Å ($g_{\rm eff} = 1.833$), and Fe I 6173 Å ($g = 2.5$, Zeeman triplet) were observed simultaneously. Fig. 1 depicts Stokes I and V profiles of the above lines. The observations are spatial averages over $0.5''$ from positions with strong V signals and are normalized to the local continuum intensity. We consider only static atmospheres, so that the reference wavelength chosen here is the (approximate) zero-crossing of the V profiles. Asymmetries in the Stokes profiles are not discussed in the present investigation.

It should be noted that, with the spatial resolution of the GCT observations used by us, which we estimate to be $0.6''$–$1.0''$, the continuum intensities in the areas with strong V signal are in the range 0.9–1.1 $\overline{I}_{\rm cont}$, where $\overline{I}_{\rm cont}$ is the average continuum intensity of the spectrogram. Thus, V signals and corresponding line gaps do not occur at particularly bright photospheric intensities (see also Kneer & von Uexküll 1991 and references therein). Below we elaborate further on this point.

3. Models of static magnetic flux tubes

We consider flux tube models, constructed using the technique outlined in HK. The method consists of solving the magnetostatic equations in the thin flux tube approximation, allowing for both radiative and convective energy transport. Using cylindrical geometry, these models treat an axisymmetric, tapered flux tube extending vertically through the photosphere and convection zone of the sun. The radiative transfer equation is solved in the eight-stream (4 angles) approximation, assuming grey opacity and local thermodynamic equilibrium. Convection is treated using mixing length theory, with an additional parameter, α, which parameterizes the inhibition of convection in the flux tube by the strong magnetic field ($\alpha = 1$ in the external atmosphere).

For reasons of consistency, a model atmosphere for the ambient medium is first constructed, assuming a non-magnetic plane-parallel atmosphere with constant vertical energy flux. We heuristically take into account deviations from a grey atmosphere in the upper photospheric layers by allowing for additional heating in the energy equation (similar to that used by Hasan, 1988). The additional flux (which never exceeds 5 % of the solar flux and which is assumed to vanish below $z = 0$), is adjusted iteratively to match the VAL C model (Vernazza et al. 1981). This term essentially reflects the error in the use of the Rosseland mean opacity in the top layers of the atmosphere, and has nothing to do with actual energy input. The "quiet sun", thus constructed, is used as the external atmosphere for calculating self-consistent models of cylindrical flux tubes that are in energy equilibrium and pressure balance with their surroundings. Similar to Hasan (1988), an additional heating rate per unit mass in the tube is taken equal to the value in the ambient medium at the same height. The influence of the ambient medium on the flux tube is taken into account by solving the radiative transfer equation along several rays that emanate from the external atmosphere and pass through the flux tube at various angles. The effects of cylindrical geometry are taken into account when solving the transfer equation. Further details can be found in HK.

The above-mentioned models treat the effects of partial ionization using Saha's equation for solar abundances and also use Rosseland mean opacities based upon the Kurucz and OPAL tables (kindly supplied by R. Kurucz).

The free parameters in the flux tube models are: α (the convective efficiency parameter), R_0 (the flux tube radius at $z = 0$) and β_0, where $\beta_0 = 8\pi p_0/B_0{}^2$ (p_0 and B_0 refer to the pressure and magnetic field strength on the flux tube axis at $z = 0$). In the present study, we choose $R_0 = 100$ km and $\alpha = 0.2$. The temperature structure of the tube is insensitive to the precise choice of α, as was demonstrated by HK. We choose a value of R_0 which is typical for photospheric flux tubes.

Figure 2 depicts the temperature and density structures of flux tube models with $\beta_0 = 1.0$ (dashed line) and $\beta_0 = 0.3$

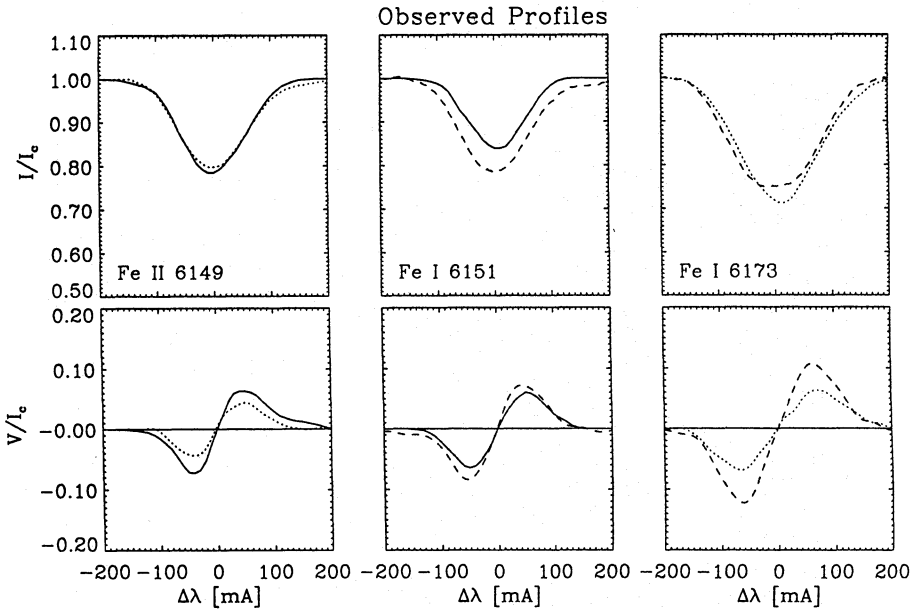

Fig. 1. Stokes I and V profiles observed with high spatial resolution in plages near disc centre, normalized to the local continuum intensity. The reference wavelengths are approximately the V zero-crossings. Profiles with the same coding, full lines, dotted, and dashed, are from simultaneous observations

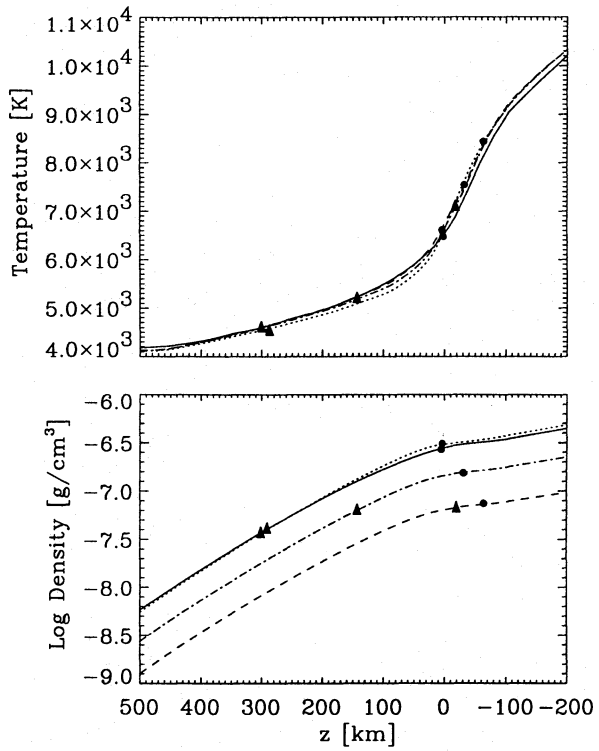

Fig. 2. Variation of temperatures and densities with geometric height in flux tube models with $\beta_0 = 1.0$ (dashed) and $\beta_0 = 0.3$ (dash-dotted) compared with the empirical VAL C model (Vernazza et al. 1981) (full curves) and the model of the ambient medium used here (dotted). The dots are at continuum optical depth $\tau_{5000} = 1$, the triangles at line centre optical depth $\tau_{6173} = 1$ of the Fe I 6173 line, calculated without magnetic field

(dash-dotted line) as functions of geometric height. We compare these with the VAL C model (Vernazza et al. 1981) for the photosphere extended into the deep layers by the model of Spruit (1977) (full curves) as well as with the model of the ambient, non-magnetic atmosphere of HK (dotted). Above $z = 0$ the flux tubes are hotter than the ambient gas by a few hundred degrees while they are cooler below $z = 0$, as discussed by Hasan & Kalkofen (1994). The temperature structure of the flux tube in the top portion of the flux tube is influenced by radiation from the ambient medium, since the optical path lengths of the rays intercepted by the flux tube are very small. However, close to $z = 0$, the effects of radiation emanating from the hot underlying layers in the tube become important, which leads to a warming of the tube with respect to its surroundings. In the present treatment, we neglect the influence of the flux tube on the ambient medium.

The models by Kalkofen et al. (1989), Pizzo et al. (1993a,b), and Grossmann-Doerth et al. (1994) take the effect of the flux tube on the surrounding medium into account, which leads to a cooling of the ambient medium. This effect may be amplified by the downflow in the non-magnetic exterior. However, the condition of radiative equilibrium for a grey atmosphere in these models leads to steep temperature gradients at low photospheric layers, much steeper than in empirical models. Furthermore, such models are unable to reproduce the observed line profiles in the quiet atmosphere. Thus, caution may be appropriate when comparing line intensities from such models with observations and drawing conclusions on flux tube properties. We note that Steiner & Stenflo (1990) have constructed non-grey static tube models, treating the radiative energy transport with opacity distribution functions, but they have not investigated the observational consequences for emergent profiles of polarized lines.

An important difference between flux tubes and the non-magnetic medium is that the flux tubes are evacuated with re-

spect to their surroundings because of the magnetic pressure. The degree of evacuation depends on the value of β. Figure 2b shows the variation of the gas density, ρ, as a function of height in the flux tube. The magnetic field strengths at $z = 0$ (assuming $\alpha = 0.2$ and $R_0 = 100$ km) are: $B_0 = 1310$ G ($\beta_0 = 1.0$), $B_0 = 1500$ G ($\beta_0 = 0.5$), $B_0 = 1600$ G ($\beta_0 = 0.3$), $B_0 = 1730$ G ($\beta_0 = 0.1$). In Fig. 2, the continuum optical depths $\tau_{5000} = 1$ and the line centre optical depths $\tau_{6173} = 1$, calculated without magnetic field, are indicated by dots and triangles, respectively, for the various models. With decreasing value of β_0, the decreased density moves the line forming layers deeper, thus to higher temperatures, which leads to increased ionization of iron and consequently a weakening of the Fe I lines.

4. Calculation of Stokes I and V profiles

The radiative transfer calculations are performed assuming LTE. For consistency with the line profiles observed in the quiet sun at disc centre, the oscillator strengths of the three lines are adjusted such that their equivalent widths calculated with the VAL C model (Vernazza et al. 1981) fit those of the Liège Atlas (Delbouille et al. 1973). For van der Waals damping the parameter C_6 is determined according to Unsöld (1955) and then multiplied by a factor of 10, as recommended by Holweger (1979).

As an example, several average observed and calculated line profiles of Fe I 6173 at quiet sun disc centre are shown in Fig. 3. The full line denotes the profile observed with the GCT, the short-dashed line is taken from the Liège Atlas. We attribute the differences in line depression to scattered light in the spectrograph of the GCT, which is independent of wavelength and amounts to 12.5 % of the continuum intensity.

This contamination by scattered light is less serious for weaker lines. For instance, for a line with true residual intensity $I_\lambda/I_C = 0.70$, a measurement would give a value of (0.70+0.125)/(1.0+0.125) = 0.733. The amplitudes of the observed Stokes V profiles, shown in Fig. 1 are too low by 12.5 %, i.e., instead of $V_\lambda/I_C = 0.10$, the corrected value is 0.1125.

The dotted profile in Fig. 3 is calculated with the VAL C quiet sun model without applying a smearing by large-scale motions, while the dash-dotted profile is obtained by a convolution of the dotted profile with a Gaussian,

$$1/(\pi^{1/2}\Delta\lambda_D)\exp(-(\Delta\lambda/\Delta\lambda_D)^2)\,,$$

where $\Delta\lambda_D = (\lambda v_{\rm macro})/c$ with $v_{\rm macro} = 1.5$ km s^{-1}. The long-dashed profile in Fig. 3 is obtained with the quiet Sun model used here for the medium surrounding the flux tubes. It is also convolved with a Gaussian with broadening corresponding to a macroturbulent velocity of 1.5 km s^{-1}.

For the emergent radiation from the flux tubes we assume that the line of sight is along the tube axis and that the inclination of the magnetic field to the vertical is negligible. As in Kneer & von Uexküll (1991) we integrate Unno's (1956) differential equations along rays at several distances from the tube axis and average the emergent I and V profiles with weights according to the annular area appropriate for each ray. In the examples considered in Sect. 5, the area filling factors at a height $z = 0$ are 0.46, 0.23, and 0.115. At the interfaces between the magnetic canopy and the ambient medium, the atmospheric parameters and the magnetic field strength are interpolated linearly.

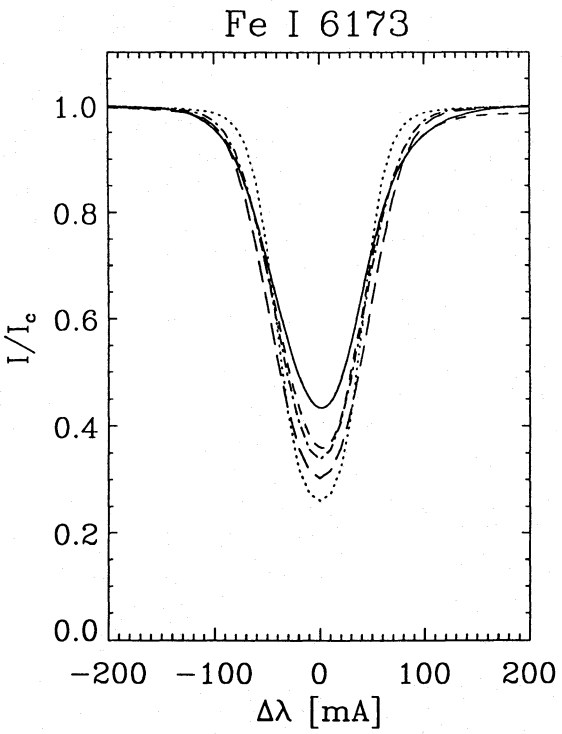

Fig. 3. Observed and calculated line profiles of Fe I 6173 at disc centre. Full profile: observed with the GCT; short-dashed: Liège Atlas (Delbouille et al. 1973); dotted: VAL C model (Vernazza et al. 1981) without macroturbulent broadening; dash-dotted: VAL C model with Gaussian broadening corresponding to 1.5 km s^{-1} (see text); long-dashed: model used here for the flux tube neighbourhood with the same macroturbulent broadening

It is reasonable to assume that magnetic flux tubes in plages are not isolated but occur in bundles. Thus, in some cases, we will assume that the magnetic field in the tube merges with that of other flux tubes in its neighbourhood at the radial distance of the outermost calculated ray. For the above filling factors this occurs at distances from the tube axis of 1.47 R_0, 2.10 R_0, and 2.49 R_0 and at heights of $z = 200$ km, 350 km, and 485 km, respectively. Above these heights the magnetic field strengths are assumed to be constant and equal to the field strength at these heights. This will be denoted therefore as 'B par' in the figures. A final free parameter is a nonmagnetic, 'microturbulent' broadening parameter, $v_{\rm mic}$, which enters the Doppler width in the absorption profiles.

5. Results

5.1. Continuum intensities

With decreasing value of the plasma β the flux tubes become more evacuated and the continuum radiation from the tube is formed at larger depth, and thus, as can be seen in Fig. 2, at higher temperature. The calculations give intensities in the tubes

that are higher than those from the quiet sun by factors of 1.72 for $\beta_0 = 1.0$ and 2.45 for $\beta_0 = 0.3$. For models compatible with the I and V profiles ($\beta_0 = 0.3$–0.5, see below), the average continuum intensities, which include also the radiation from the ambient medium, are higher than the quiet sun intensity by factors of 1.25–1.65. This disagrees with the observation that the continuum intensities at places with strong V signal are not noticably higher than average (cf. Sect. 2 above and the discussion of the line gap phenomenon in Kneer & von Uexküll 1991). But in the context of the present modeling these high intensities are unavoidable. They are a consequence of the use of a model of the undisturbed quiet sun for the ambient medium.

A remedy for the difference between the computed continuum intensities with the observed intensities might be to use cool ambient medium models like the ones mentioned in Sect. 3. In these models, the temperature gradient in the tube at continuum and line forming layers is reduced (cf. Fig. 3 in Kalkofen et al. 1989, and Fig. 1 in Grossmann-Doerth et al. 1994). We return to this feature below.

5.2. *Stokes I and V profiles*

Figure 4 compares calculated I and V profiles from the $\beta_0 = 1.0$ tube model with observations. Here and in the remaining figures the three area filling factors given in Sect. 4 are used. No broadening of the I profiles, i.e., convolution with a Gaussian, was applied. It is seen that the separation of the V extrema of the computed Fe I lines is insufficient to match the observations. Apart from this, the I profiles are too deeply depressed for any reasonable filling factor. A filling factor much larger than 50 % for the flux tube (at $z = 0$) would somewhat weaken the I profiles, but would yield V amplitudes that are too large. The reason is that the I profiles from the tube alone already give absorption that is too strong. This discussion shows the advantage of using both the observed I profiles and the V profiles as diagnostics.

Weaker absorption in the computed Fe I lines is obtained for a lower value of β_0, i.e., for a higher temperature and thus a higher degree of ionization of iron. The case of $\beta_0 = 0.1$ (not shown) must be ruled out since the model is so hot that only little neutral iron is left and hence the V amplitudes would be far too low. Thus, because of the effect of the temperature on the degree of ionization of iron we reach the same conclusion as Rüedi et al. (1992) who determined from 27 V spectra with low spatial resolution of an infrared line pair a histogram of β values that peaks at $\beta \approx 0.3$. Substantially lower values are not found.

In the remaining calculations the parameter 'B par' was used. The I and V profiles of the three lines are formed in fairly deep layers and are therefore insensitive to the merging of magnetic fields above $z = 200$ km. Fig. 5 shows the comparison of observed and calculated profiles for the case $\beta_0 = 0.3$. Compared to the case of $\beta_0 = 1.0$ (Fig. 4), the resulting profiles are in better agreement with the observed profiles. However, the I profile of the Fe II line is still too deeply depressed. Increasing the temperature does not lower the relative density of ionized iron. On the other hand, a lower temperature *gradient* would lead to better agreement since it would yield a lower line depression and lower V amplitudes. Apart from the failure to match the Fe II observations, the model gives Fe I I profiles that are too narrow and show too small a separation of their V extrema. On the other hand, the separation in the Fe II 6149 line, which has the smallest Landé factor of the three lines, is satisfactory.

To test the influence of nonmagnetic broadening we increased the microturbulence in the tube to 2.5 km s^{-1}, keeping $\beta_0 = 0.3$. The Fe I lines are weak in the flux tube models, while the Fe II line is marginally weak, giving $W_\lambda = 25$ mÅ; thus microturbulent and macroturbulent broadening are essentially equivalent. The results are shown in Fig. 6: The I profiles of the Fe I lines have changed only little, while their V profiles are indeed broader, but also with lower amplitude than for the case of $v_{\rm mic} = 1.0$ km s^{-1}. At the same time, Stokes V of the Fe II line also has become broader. Now the separation of the V extrema of this weakly split line is too large. This argues against nonmagnetic broadening by "turbulent" velocities and for broadening proportional to the Landé factor, i.e., magnetic broadening. This may possibly occur when the magnetic field within the observed area has temporarily increased field strength in the line forming layers that is larger than that of the static model. Modeling this case would require time-dependent flux tube models.

Our finding here is in strong disagreement with results from observations with low spatial resolution in the infrared by Zayer et al. (1989) and Rüedi et al. (1992). Using line pairs of very different magnetic sensitivity they also separated magnetic from non-magnetic broadening. They found that the spreading of the flux tube with height is sufficient to account for the magnetic broadening, while a substantial "macroturbulent" Doppler broadening of 2–3 km s^{-1} is needed to match the observed V profiles. Such high velocities, however, are not (yet) seen in high spatial resolution observations (e.g. Amer & Kneer 1993) such as those discussed in this paper, where only velocities that are lower by a factor 4 are observed. We therefore caution against interpreting this profile fitting parameter as physically real. It is not clear whether modeling of the infrared lines with reduced Doppler broadening but with additional magnetic field fluctuations would give V profiles incompatible with measured profiles. We believe that the discrepancy can only be resolved by observations with very high spatial resolution.

As our last example we show in Fig. 7 the I and V profiles for the choice of $\beta_0 = 0.5$ with $v_{\rm mic} = 2.5$ km s^{-1}. Compared to the case of $\beta_0 = 0.3$, both the line absorption and the V profiles of the Fe I lines are stronger as a consequence of the lower ionization of iron. Within the framework of the static flux tube models embedded in the quiet sun, the model with $\beta_0 = 0.5$ gives the best agreement with observed profiles. However, the separation of the computed V extrema of Fe II 6149 disagrees with observations, indicating that the microturbulent broadening is too large.

Finally, we note that an area filling factor for the flux tube at height $z = 0$ in the range of 25–50% is compatible with the observations. The lower limit, however, gives line absorption that is too strong for all three lines and a V signal of the Fe I 6151 line that is too weak. It is not clear whether 25–50 percent of

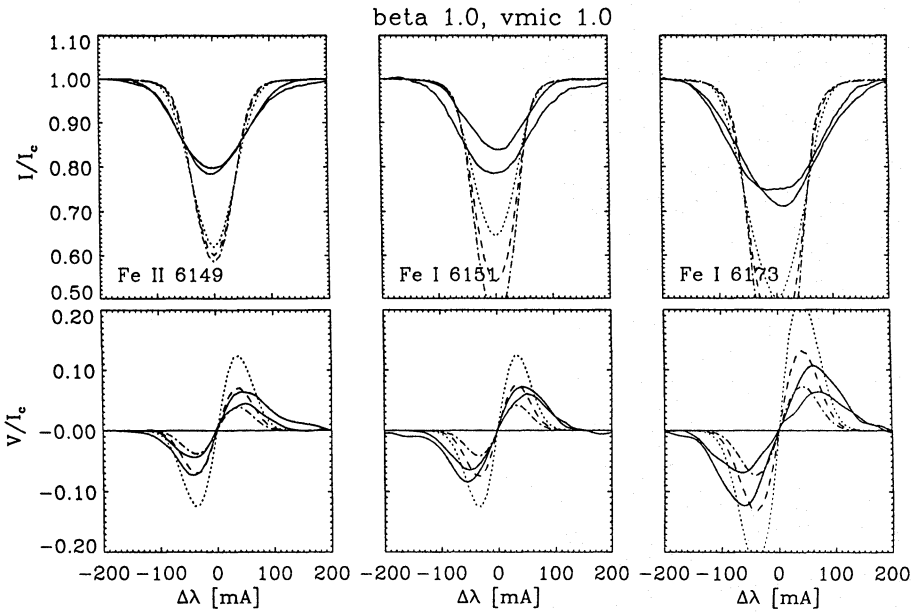

Fig. 4. Comparison of calculated Stokes I and V profiles from flux tube models with β_0 = 1.0 with observation. Dotted: filling factor 0.46 at z = 0; dashed: filling factor 0.23; dash-dotted: filling factor 0.115; full profiles: observed, see Fig. 1 for simultaneously observed profiles. The microturbulent broadening $v_{\rm mic}$ in the tube corresponds to 1.0 km s^{-1}

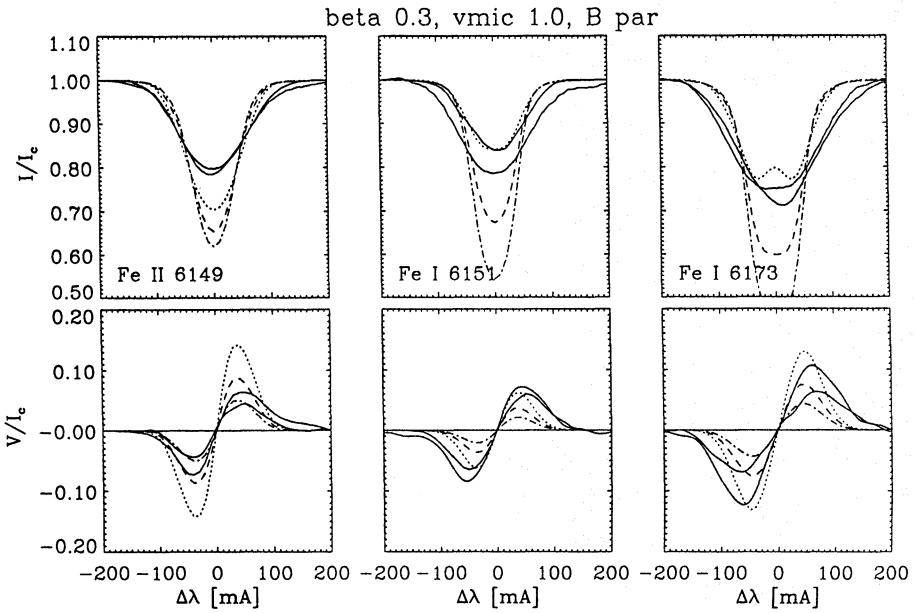

Fig. 5. Stokes I and V profiles from flux tube models with β_0 = 0.3, again compared with observation. The coding of the curves is the same as in Fig. 4. See the text for the parameter 'B par'

the area can be filled with a single flux tube, which then would have a diameter on the order of 200–400 km according to the estimated spatial resolution of our observations. A configuration with nests of densely packed smaller tubes is plausible as well. Nests of bright facular points in plages have been observed by de Boer & Kneer (1992), although these authors could not measure magnetic field signatures.

6. Discussion and conclusions

We have calculated Stokes I and V profiles of Fe I and Fe II lines with different sensitivity to temperature and magnetic field strength emerging from models of small-scale magnetic flux tubes and have compared them with observations of high spatial resolution. The flux tubes are static and their temperature structure is dominated by the radiation field from the ambient medium for which a model of the quiet sun was taken.

We found it advantageous to use both the V and the I measurements for comparison of the model predictions with observations. The I and V profiles are both sensitive to the temperature structure and to the area filling factor of the flux tube, which greatly limits the choice of possible parameter combinations. We found, in agreement with Rüedi et al. (1992), that models with plasma β in the range of 0.3–0.5 agree best with the observations. The weakening of spectral lines, or the line gap phenomenon, which is seen best in high resolution spectrograms of plages and which is especially pronounced in Fe I lines, appears as a consequence of both the magnetic line splitting and the high temperature, and thus high ionization degree of the flux tube gas.

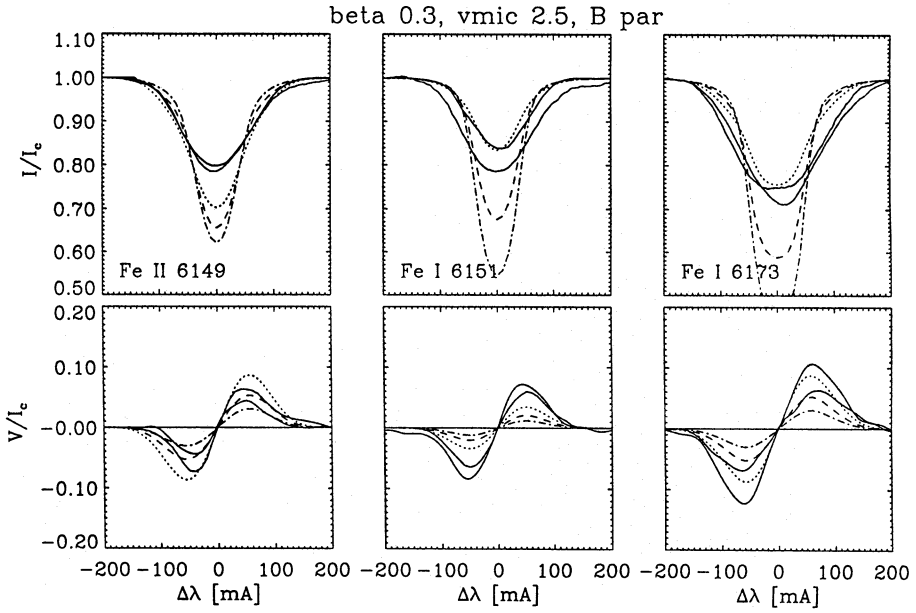

Fig. 6. Observed and calculated Stokes I and V profiles. $\beta_0 = 0.3$, $v_{\rm mic} = 2.5$ km s^{-1}. The coding of the curves is the same as in Fig. 4

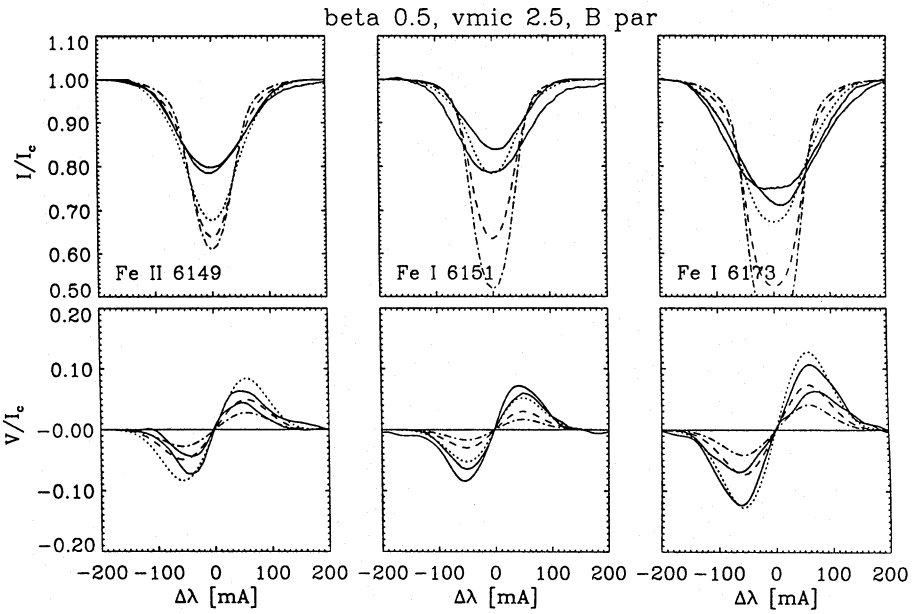

Fig. 7. Observed and calculated Stokes I and V profiles. $\beta_0 = 0.5$, $v_{\rm mic} = 2.5$ km s^{-1}. The coding of the curves is the same as in Fig. 4

To obtain sufficient separation of the Stokes V extrema of strongly split lines, some additional broadening beyond that from the static magnetic field is necessary. However, a strong, "turbulent" velocity field yields too widely separated V extrema of weakly split lines. We would thus prefer models with intermittently strong magnetic fields, larger than the field of static flux tubes at a fixed depth. Such models must be dynamic, similar to those calculated, amongst others, by Hasan (1991) and Steiner et al. (1994). In that case the broadening is proportional to the Landé g factor, which is required by the observations. (But see Zayer et al. 1989 and Rüedi et al. 1992.)

The two major limitations of our models are: Firstly, they do not reproduce the observed continuum intensities. It is well known that, apart from pores, magnetic features in plages do not show any conspicuous intensity contrast even if only moderately averaged over 0.6″–1.0″(cf. Kneer & von Uexküll 1991 and references there, as well as Amer & Kneer 1993). It is inherent in our tube models embedded in an unperturbed quiet sun model as the ambient medium that the continuum intensity from the average of the tube and the surrounding atmosphere is always higher than the quiet sun intensity. This discrepancy can be removed only by reducing the temperature of the ambient medium below that of the undisturbed quiet solar atmosphere, which reduces the temperature also within the tube and yields lower continuum intensities from the tube as well as lower average intensities. Such a temperature reduction is obtained in the 2-D slab models of Kalkofen et al. (1989) and Grossmann-Doerth et al. (1994), where radiative back reaction of the tube on the ambient gas is taken into account.

At the other extreme, very low values of continuum intensities in the flux tube, with a factor of about 0.9 lower than those from the quiet Sun, were deduced from low spatial resolution spectra by Solanki & Briglević (1992) and Grossmann-Doerth et al. (1994). We disagree with this result, which may be based on taking averages over features with different structure, such as small-scale tubes and larger pores (see the discussion in Solanki & Briglević 1992). The objection lies in the following: Small-scale magnetic elements, on average, require a cool ambient gas nearby since otherwise the gas in the tube is heated too much, yielding *average* continuum intensities higher than those seen in high resolution spectrograms. If, in addition, the continuum radiation from the tube proper is lower than that from the quiet sun, the intensity average from the flux tube and the ambient atmosphere may become lower than that observed.

Secondly, in addition to a general reduction of the temperature, a lowering of the temperature *gradient* appears to be necessary for a better match of the I and V profiles of Fe II, i.e., for a reduction of the absorption and the V signal calculated from the models. We expect that the effect of increased absorption and an increased V signal in Fe I lines from tubes with reduced temperature is counteracted by the lower temperature gradient.

The need for both reduced temperature along the whole tube and reduced temperature gradient is in full accord with the earlier result by Keller et al. (1990). Their empirical models, deduced by an inversion procedure, clearly exhibit both features. Yet again, as in the work of Zayer et al. (1989) and Rüedi et al. (1992), in order to fit the width of the V profiles, a large Doppler broadening parameter of 1.3–3.0 km s^{-1}, this time dependent on the spectral line, had to be introduced. This feature is not reflected in observations with high spatial resolution.

In this paper, the approach to the investigation of flux tube structure is different from that of derivations of empirical models via low resolution observations of Stokes V profiles. We determine the run of temperature from the energy equation in which the radiation transport plays the dominant rôle (Deinzer et al. 1984a, b). In order to reduce as much as possible a dependence on free parameters, such as the area filling factor and macroturbulence, we use high spatial resolution observations of I and V profiles for comparison with the radiation emerging from flux tubes models. We are reluctant to accept turbulent velocities of a significant fraction, of 30–50 percent say, of the tube speed (which is composed of the sound velocity and the Alfvén velocity and is about a factor 0.7 lower than the sound velocity in the flux tube layers considered). Such large gas motions, either stationary or in waves, have a strong impact on the internal tube structure at all heights. Our modeling suggests that flux tubes are dynamic, which is also shown in the above-mentioned work by Hasan (1981) and Steiner et al. (1994), and that they are very likely inhomogeneous in the horizontal direction. We also admit that the observations with which we deal here fall far short of resolving the shape of flux tubes. Very high angular resolution polarimetry is urgently needed.

To obtain an appropriate temperature structure within the tube model requires taking the effect of the flux tube on the ambient medium into account. We fully agree with the statement of Bünte et al. (1993) that the structure of the surrounding medium is an essential part of understanding the various tube phenomena. These authors performed a sophisticated modeling with arrays of flux tubes in an external flow field to explain the centre-to-limb variation of the asymmetry of the V profiles. The temperature and gas density inside and outside the tubes were taken from empirical models. But the more the outside dynamic behaviour resembled our picture of granular convection (warm, broad, upward flow at some distance from the tubes; horizontal flow towards the tubes; and cool, fast downflow close to the tubes) the better the observed line asymmetry was reproduced. Here we found the outside cooling flow necessary from the requirements for the temperature structure inside the tubes, namely low temperatures in the deep layers, lower than the average subphotospheric temperature.

By focussing on the discrepancies between the theoretical and observed Stokes profiles, our analysis points to possible directions in which models can be improved. We expect to incorporate further refinements to our models in forthcoming investigations.

Acknowledgements. We thank Prof. J.O. Stenflo, the referee, for his supporting recommendations. The Gregory Coudé Telescope is operated by the Universitäts-Sternwarte Göttingen at the Spanish Observatorio del Teide/Tenerife of the Instituto de Astrofísica de Canarias.

References

Amer M.A., Kneer F., 1993, A&A 273, 304
Auffret H., Muller R., 1991, A&A 246, 264
Bünte M., Solanki S.K., Steiner O., 1993, A&A 268, 736
de Boer C.R., Kneer F., 1992, A&A 262, L24
Deinzer W., Hensler G., Schüssler M., Weisshaar E., 1984a, A&A 139, 426
Deinzer W., Hensler G., Schüssler M., Weisshaar E., 1984b, A&A 139, 435
Delbouille L., Roland G., Neven L., 1973, Atlas Photométrique du Spectre Solaire de λ3000 à λ10000, Institut d'Astrophysique de l'Université de Liège, Cointe/Ougrée
Grossmann-Doerth U., Knölker M., Schüssler M., Solanki S.K., 1994, A&A 285, 648
Hasan S.S., 1988, ApJ 332, 499
Hasan S.S., 1991, in: Ulmschneider P., Priest E.R., Rosner R. (eds.) Chromospheric and Coronal Heating Mechanisms. Springer, Berlin, p. 408
Hasan S.S., Kalkofen W., 1994, ApJ 436, 355
Holweger H., 1979, in: Proc. XXIInd Liège International Astrophysical Symposium, Institut d'Astrophysique. Liège, p. 117
Kalkofen W., Bodo G., Massaglia S., Rossi P., 1989, 2D Flux Tube in Radiative Equilibrium. In: Rutten R.J., Severino G. (eds.) Solar and Stellar Granulation. Kluwer, Dordrecht, p. 571
Keller C.U., Solanki S.K., Steiner O., Stenflo J.O., 1990, A&A 233, 583
Kneer F., Uexküll M. von, 1991, A&A 247, 556
Koutchmy S., 1977, A&A 61, 397
Pizzo V.J., MacGregor K.B., Kunasz P.B., 1993a, ApJ 404, 788.
Pizzo V.J., MacGregor K.B., Kunasz P.B., 1993b, ApJ 413, 764.
Rüedi I., Solanki S.K., Livingson W., Stenflo J.O., 1992, A&A 263, 323

Schüssler M., Schmidt W., 1994, Solar Magnetic Fields, Proc. Intern. Conf. held in Freiburg, June 29–July 2, 1993. Cambridge University Press, Cambridge

Solanki S.K., 1995, Magnetic Field Measurements in the Infrared. In: Kuhn J., Penn M. (eds.) Proc. 15th Sacramento Peak Workshop, 1994, Infrared Tools for Solar Astrophysics: What's Next? Sunspot, NM, in press

Solanki S.K., Briglević V., 1992, A&A 262, L29

Spruit H.C., 1977, Ph.D. thesis, Utrecht University

Steiner O., Stenflo J.O., 1990, Model Calculations of the Photospheric Layers of Solar Magnetic flux tubes. In: Stenflo J.O. (ed.) Proc. IAU Symp. 138, Solar Photosphere: Structure, Convection and Magnetic Fields. Kluwer, Dordrecht, p. 181

Steiner O., Knölker M., Schüssler M., 1994, in: Rutten R.J., Schrijver C.J. (eds.) Proc. International Conference, Solar Surface Magnetism. Kluwer, Dordrecht, p. 441

Stenflo J.O., 1994, Solar Magnetic Fields — Polarized Radiation Diagnostics. Kluwer, Dordrecht

Unno W., 1956, PASJ 8, 108

Unsöld A., 1955, Physik der Sternatmosphären. 2nd ed., Springer, Berlin

Vernazza J.E., Avrett E.H., Loeser R., 1981, ApJS 45, 635

Zayer I., Solanki S.K., Stenflo J.O., 1989, A&A 211, 463

This article was processed by the author using Springer-Verlag LaTeX A&A style file version 3.